

## CHAPTER II

### THEORETICAL BACKGROUND AND LITERATURE REVIEW

#### 2.1 Clay Chemistry

##### 2.1.1 Structure and Properties of Clay

Clay minerals are the 'layer types' inorganic fillers differentiated by the number of tetrahedral and octahedral sheets that have combined and the types of isomorphic substitution of the cations (Bandi, 2006). One the most commonly used layered silicates is sodium montmorillonite ( $\text{Na}^+$ -MMT) belonging to the family of 2:1 phyllosilicates.  $\text{Na}^+$ -MMT has a granular appearance with a particle size in the micron order (10-50  $\mu\text{m}$  in diameter). Its crystal structure consists of two silicon oxide tetrahedral sheets fused to an aluminium or magnesium hydroxide octahedral sheet, as depicted in Figure 2.1. The thickness of each platelet is about 1 nm and its lateral dimension may vary from 30 nm to several microns or larger, depending on the particular silicate layers.

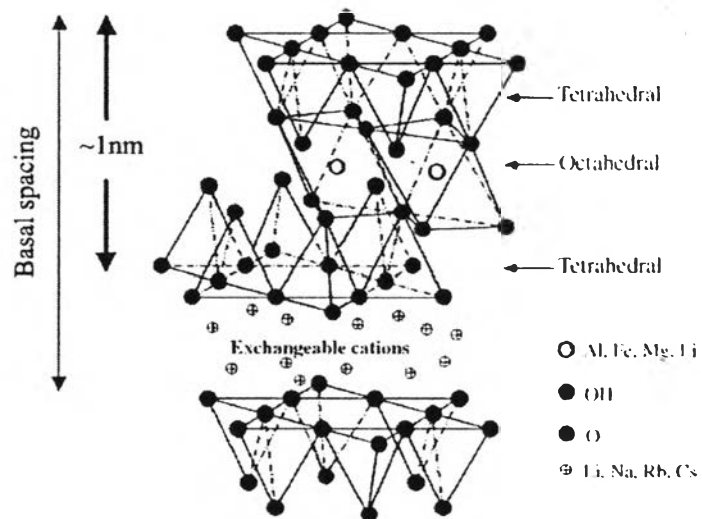


**Figure 2.1** The crystal structure of the  $\text{Na}^+$ -MMT.

Stacking of the layers leads to a regular van der Waals gap between the layers called the 'interlayer or gallery'. The isomorphic substitution of  $\text{Si}^{4+}$  by

$\text{Al}^{3+}$  within the tetrahedral sheet and  $\text{Al}^{3+}$  by  $\text{Fe}^{2+}$  or  $\text{Mg}^{2+}$  within the octahedral sheet produces the negative charges that are counterbalanced by the alkali or alkali earth cations, situated inside the galleries. However, in the case of tetrahedral substitution, the excess negative charge will be localized much nearer to the periphery of the siloxane surface, providing much stronger adsorption complexes with either interlayer cations or polymer matrices compared to that of octahedral substitution. In this regard, the layer surfaces are available for the hydration and ion exchange reactions with organic or inorganic cations e.g. primary, secondary, tertiary, and quaternary alkylammonium cations or phosphonium cations to render the organophilic, which will be further utilized for the preparation of polymer nanocomposites. Further, the alkylammonium or alkylphosphonium cations may provide the functional groups that can interact or react with the polymer matrix, or in some cases initiate the polymerization of monomers, situated inside the galleries, to improve the adhesion between the clay and polymer matrix (Mai and Yu, 2006).

Swelling of smectite clays occurs through the adsorption of the water molecules in the interlayer region through the separation of clay particles. Thus, the layer swell not only longitudinally but also laterally, independent of the water content, which is consistent with a zig-zag column model (Bandi, 2006). The swelling mechanisms can be differentiated into two types depending on the growth of the basal spacing. The first one is crystalline swelling, being as a result of the adsorption of monolayers of water on the basal crystal surfaces, whereas the second type is the osmotic swelling, which mostly depends on ionic concentration, type of counter-ion, pH of pore water, and type of clay (Bandi, 2006). Montmorillonite saturated with polyvalent cations cannot expand its interlayer separation beyond  $10\text{\AA}$ , since the inter-platelet repulsive force is offset by the electrostatic attraction between the silicate layers and cations. However, montmorillonite saturated with monovalent cations e.g.  $\text{Na}^+$  or  $\text{K}^+$  is strongly hydrated and exhibits a greater degree of platelet separation when swelling in water. This can be explained by the much stronger inter-platelet repulsion as compared to the electrostatic attraction, which in turn promotes the expansion of the interlayer spacing from ten to hundred of Angstroms. It should be noted that the lack of interlayer counter-ions will affect the ability to swell and disperse in water.

The thermodynamically stable gel, resembling a ‘house of cards’, can be formed when the clay concentration in water exceeds the critical gelling concentration, which is around 2 wt%. As there is the opposite surface and edge charges existing in a single layer structure, three different modes of associations are preferred for the gelation: face to face (FF), edge to face (EF) and edge to edge (EE), as illustrated in Figure 2.2. It is believed that the house of cards structure or stable gel network is developed throughout the electrostatic interaction between the negatively charged faces and positively charged edges, followed by rearranging themselves to minimize free energy. This signifies that the structure of clay gel does not comprise the individual platelets but instead appears as the long range orientation of clay stacks, which are held together by hydrated counter-ions. Further, it is possible that the repulsive force between the platelets will be restrained by the frictional forces created by the interactions between clay particles via edge to face bonds during the swelling water. This might limit the degree of platelet separation.

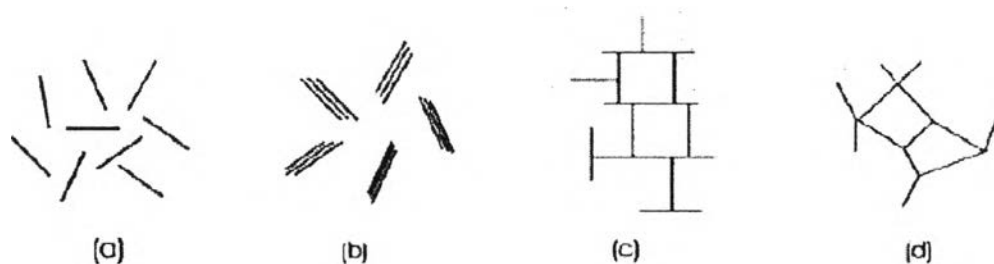


**Figure 2.2** Modes of particle association in clay suspensions: (a) dispersed; (b) face-to-face FF; (c) edge-to-face EF; and (d) edge-to-edge EE.

### 2.1.2 Clay Aerogel

The term ‘aerogel’ is used to describe a typical inorganic material with high porosity (~98%), high specific surface area ( $> 1000 \text{ m}^2\text{g}^{-1}$ ), and bulk density less than  $0.1 \text{ gcm}^{-3}$ . The most studied aerogels are those of silica, which were first reported by Kistler since 1931 (Kistler, 1931). These aerogels usually require

precursors that are first capable of being hydrolyzed and then condensed to form a wet gel, followed by a removal of liquid phase in the gel by using either a supercritical CO<sub>2</sub> drying or freeze-drying technique. Unlike the above mentioned aerogels, clay aerogels can be formed in one step with water through the freeze-drying process without involving the chemical condensation route. Freezing the stable clay gel will produce the lamellar structure, whose dimensions are strongly dependent on the temperature of nucleation and freezing rate (Gawryla, 2009a).

Clay aerogel is a representative of an emerging class of structural materials with ultra-low density, high porosity, and low thermal conductivity, which is similar to the conventional polymeric foams. It stands out as a good candidate for a wide variety of applications starting from thermal/acoustical insulation till drug delivery and biomedical applications, depending on the constituent materials, which makes up the layered superstructure. The freeze-drying process represents as the environmentally benign technique for creating the light-weight materials alternatives to the typical polymeric foams. The lamellar structure is therefore a replica of the ice crystal morphology, which grows in the direction from edge toward the center of vial i.e. in the direction of temperature gradient. This is explained by the fact that when an aqueous solution of dispersed particles is frozen, the non-solvent materials or impurities will be excluded from the growing ice crystals and aggregate at the grain boundaries between individual ice crystals. If the interaction between these impurities; for instance, edge to face (EF) conformation of the clay platelets, is strong enough, the final structure will be retained upon the removal or sublimation of ice crystals, as shown in Figures 2.3 and 2.4. The temperatures at which the clay gel is frozen affect the size scale of the internal structure. For instance, by freezing at the temperature of liquid nitrogen, this creates sub-micron to micron thick layers with spacing between layers in the range of ten to hundred of microns, while freezing at temperatures just below the melting point of water provides the several microns in thickness and millimeter scale spacing. The larger spacing is explained by the fact that each growing crystals have more time to move the impurities out of the crystal growth path (Gawryla, 2009a). It should be noted that a room temperature drying of the frozen clay solution does not produce the house of card structure, but instead restores the original clay morphology.

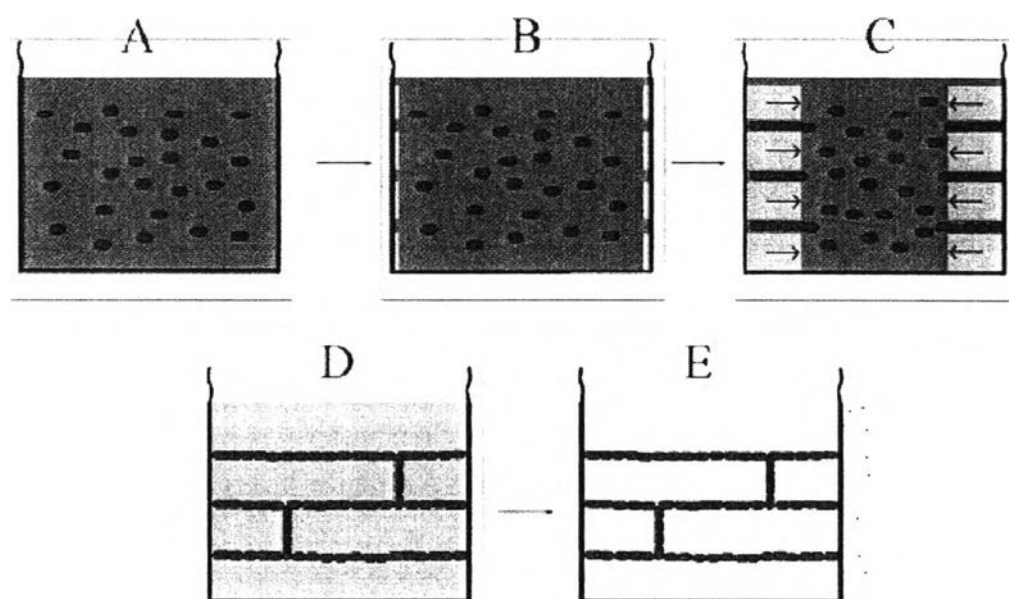


**Figure 2.3** (A) Stable gel; (B) Nucleation at the edge of the vial; (C) Ice growth toward the center of vial; (D) Frozen solution; (E) After sublimation (Gawryla, 2009a).

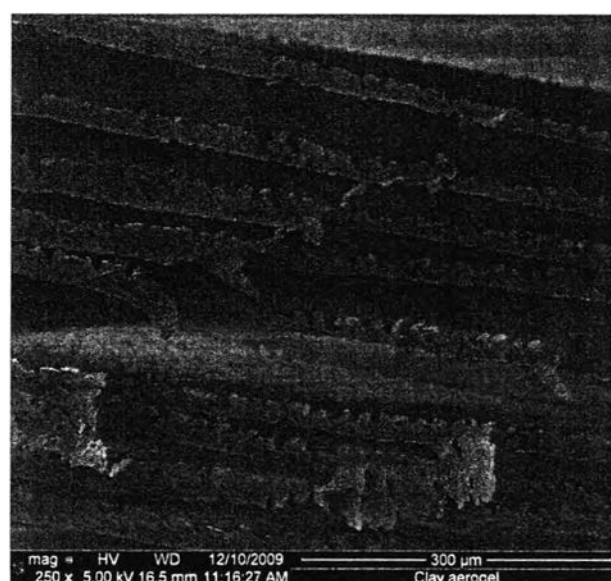


**Figure 2.4** SEM micrograph of the clay aerogel.

The structure and properties of the ice-templated materials can be tailored by manipulating the experimental variables viz. types and concentrations of clays, molecular weight (MW) and chemistry of reinforcing polymers, directionality of ice crystallization, mold design, orientation of the microstructure, freezing temperature, and the existence of other reinforcing fillers. Each scenario is discussed in detail as follows:

#### 2.1.2.1 Effect of Clay-Clay Interactions

A particular grade of clay exhibits a unique chemical nature in terms of the exchangeable cations, aspect ratio as well as the critical concentration for forming a stable structure after being freeze-dried. The influence of concentrations and compositions of clays on the structure formation is summarized in Table 2.1. It is seen that the ion exchange capacity (CEC) and aspect ratio do affect the ability to form the three dimensional network structure; for instance, Na<sup>+</sup>-MMT forms a well defined structure, when its concentration is above 2 wt%, whereas kaolin, which interacts less strongly as compared to Na<sup>+</sup>-MMT, do not form a stable structure at low concentration unless above 20 wt%. In brief, a high aspect ratio coupled with a high CEC produces the most stable structure after freeze-drying.

**Table 2.1** Comparison between the critical concentration for forming the stable structure (Gawryla, 2009a)

Samples	Concentration	Outcome
Na <sup>+</sup> -MMT	< 2 wt%	Expanded powder
Na <sup>+</sup> -MMT	> 2 wt%	Layered structure
Ca <sup>2+</sup> -MMT	≤ 5 wt%	Expanded powder
Fluoromica	5 wt%	Layered structure
Kaolin	≤ 5 wt%	Expanded powder
Kaolin	20-50 wt%	Layered structure
Laponite	5 wt%	Layered structure

### 2.1.2.2 *Effect of the Molecular Weight (MW) and Chemistry of the Reinforcing Polymers*

As a result of this architecture, the neat clay aerogel is relatively fragile and difficult to handle without damaging its structure. It is therefore of particular importance to reinforce the clay aerogel framework with the polymeric components to produce the more stable structure. This can be accomplished by using several types of polymers; for instance, temperature-responsive polymers (Bandi, 2006), water-soluble polymers (Bandi, 2006; Finlay *et al.*, 2008; Gawryla, 2009a), thermosetting polymers (Arndt *et al.*, 2007), biodegradable polymers (Gawryla, 2009a), etc. In addition to the reinforcing effect, the microstructure of the foam-like materials can be tailored by changing the weight fraction and molecular weight of the polymer. Increasing the weight fraction of polymer leads to a structural change from a highly lamellar morphology, in which layers distinctly separate, to a more continuous structure, in which the layers are connected by a web of polymer. This allows for perfection of the foam-like structures and creates the effective load transfer under the applied stress, resulting in the vastly improved mechanical behaviors. On the contrary, there is a transition from the highly lamellar to a disordered type structure upon increasing the molecular weight of polymer. This is explained by the fact that the hydrodynamic radius increases with the molecular weight of polymer, which means that the larger polymer can interact with more than one clay platelet and forms a dense gel network that further prevents the long ice crystals from growing. As a result, a new ice crystal is nucleated on the other side of the network, producing a random structure (see Figure 2.5). For this reason, the isotropic structure, produced at the high molecular weight, exhibits a lower mechanical strength due to the lack of the small web-like reinforcements for preventing the layers from bending, as compared to that of the lamellar morphology with a web-like substructure.

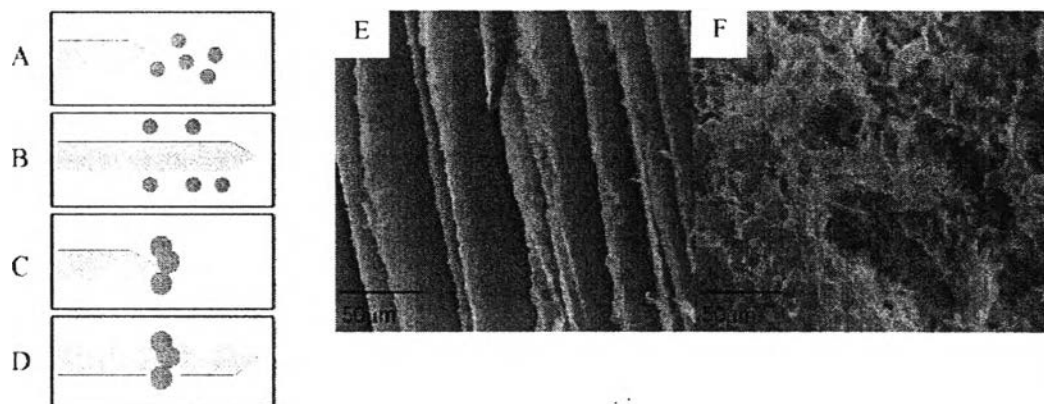


**Figure 2.5** The growth of ice crystals as a function of molecular weight of the polymer: (A, B) low molecular weight; (C, D) high molecular weight. SEM images of polymer/clay aerogel composites: (E) lamellar structure; (F) disordered structure (Gawryla, 2009a).

### 2.1.2.3 Effect of the Processing Methods

It was demonstrated that changing the direction of ice growth, thereby the alignment of the layers, affects the properties of ice-templated materials in terms of the mechanical integrity and thermal conductivity. The direction of ice growth can be controlled by using either the controlled nucleation points or the directional freezing method viz. in a vertical or horizontal manner. By using the vertical freezing technique, a highly anisotropic material, having high strength in the grain direction but not in the other two directions, will be created and displays the expected decrease in thermal conductivity (Gawryla, 2009a). However, when the samples are frozen within the cylindrical polystyrene (PS) vials, the nucleation and orientation of the ice crystals are no longer controlled. This results in regions, where the layers are aligned within the same direction, though the entire material has several such domains randomly oriented with respect to each other. At the same time, when a freeze-thaw process is repeated three times before being freeze-dried, the number of domains with smaller effective length will be increased, while the sample does not undergo any change in size (density). This restructuring leads to a more isotropic structure (see Figure 2.6) that is much stronger than the one with fewer



large domains, as the forces are now distributed among many smaller regions. Besides, the thickness and space between layers can be tailored through freezing at different temperatures. A large super-cooling signifies a rapid nucleation and fast propagation of the ice crystals, thus limiting the movement of the impurities or solid particles before being trapped at the grain boundaries. Thus, the small size scale is created. On the contrary, freezing at higher temperature provides a much larger spacing, as the impurities have more time to be moved out of the crystal growth direction.

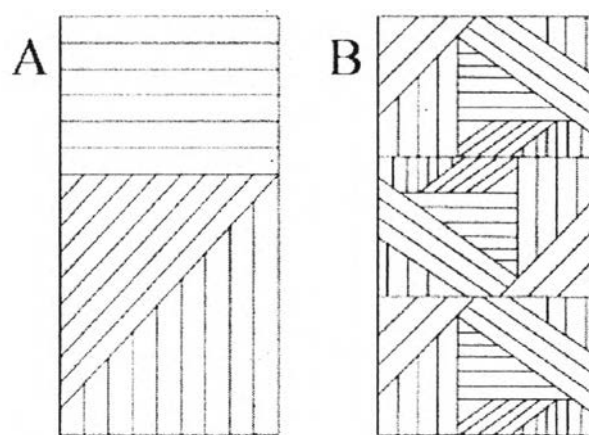


**Figure 2.6** (A) Randomly nucleated; (B) Cryostructured structures (Gawryla, 2009a).

#### 2.1.2.4 Effect of the Incorporation of Other Reinforcing Fillers

Similarly, the properties and microstructure of the pristine clay aerogel can be tailored by adding the other reinforcing fillers such as biologically-based fibers and single-walled carbon nanotubes (SWCNT). For instance, the compressive modulus was increased from 14 to 1800 kPa upon the addition of 5 wt% short-cut silk fiber into the initial clay gel (Finlay *et al.*, 2008). This was explained by the formation of woven-like structure with clay layers and reinforcing fibers in the warp and weft directions, respectively. Aerogels that comprises both  $\text{Na}^+$ -MMT and cellulose nano-fibers exhibited the compressive strengths that were significantly higher than predicted by a simple additive behavior of the properties of the individual

components, especially if only a small fraction of the minor component was added (Gawryla *et al.*, 2009b). This was due to a synergistic effect of the clay-whisker combination; that is, the three dimensional network structures were achieved with dispersions comprising the ingredients in concentrations that individually would not allow one to produce such structures. In other words, a nano-scale ‘wattle-and-daub’, in which the mud-like clay and straw-like cellulose whiskers complement each other, was produced and promoted the load transfer under stress. Increasing the content of the minor component beyond a point where a substantial increment in stiffness was reached had a small effect on the materials stiffness, but rather increased the overall bulk densities.

In addition to the reinforcing benefits, it was found that the electrical conductivity of the aerogels, comprising poly(acrylic acid) (PAA) and Na<sup>+</sup>-MMT can be fine-tuned by changing the pH and mass fractions of the single-walled carbon nanotubes (SWCNT) of the aqueous solutions prior to freeze-drying without affecting the lamellar structure (Gawryla *et al.*, 2009c). The shear forces, imparted by the growing ice crystal, were capable of creating a better alignment of the SWCNT, hence providing an appreciable electrical behavior even at very low SWCNT concentration, as shown in Table 2.2. Further, while the SWCNT reinforced the materials, a significant increase was evidenced when using the aqueous solution at high pH, where the nanotubes were strongly networked into their bundled state and conferred a great resistance to the bending.

The firing process can be considered as an approach to improve the mechanical properties of the ice-templated materials; for instance, the fired clay aerogel exhibited the compressive modulus of 700 kPa, which is about 25 times higher than that of the native one (Gawryla, 2009a). However, the out-coming layers are much thinner and unable to support their own weight, thereby resulting in the collapse and shrinkage of the lamellar structure. The extent of shrinkage is also dependent on the firing temperature as well as duration of firing, as depicted in Figure 2.7.

**Table 2.2** Aerogels electrical conductivity (Gawryla *et al.*, 2009c)

Samples	Electrical conductivity ( $\text{Scm}^{-1}$ )
2.5% PAA, pH = 3	$8.36\text{E-}06 \pm 3.72\text{E-}06$
2.5% PAA, 5% clay, pH = 3	$1.67\text{E-}06 \pm 4.89\text{E-}07$
0.5% PAA, pH = 3	$1.63\text{E-}04 \pm 4.1\text{E-}05$
0.5% PAA, 5% clay, pH = 3	$9.45\text{E-}05 \pm 5.8\text{E-}05$

<sup>a</sup> The content of SWCNT was kept constant at 0.05 wt%.

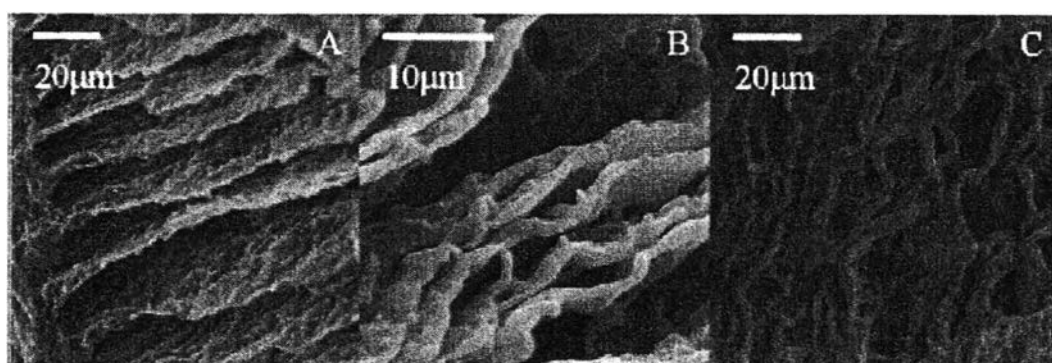


**Figure 2.7** SEM micrographs of the fired clay aerogel: (A) at 850°C for 1 hr; (B) 900°C for 1 hr; (C) 900°C for 3 hr (Gawryla, 2009a).

## 2.2 Elastomer Nanocomposites

### 2.2.1 Overview of Natural Rubber (NR)

NR latex is a stable colloidal dispersion of *cis*-1,4-polyisoprene obtained from the *Heavea Brasiliensis* tree. The field latex contains approximately 33% of rubber content and is usually concentrated to 60% rubber by a process called centrifugation in order to remove part of the undesired serum and to attain the

uniformity of the product. The concentrated latex is either preserved with ammonia or mixture of ammonia, zinc oxide and tetramethylthiuram disulfide (TMTD) for preventing the bacterial growth after centrifugation, so it will be used as raw materials for NR latex products. Apart from the rubber hydrocarbon particles, the field latex contains small amounts of fatty acids and proteinaceous substances; which is verified to be potential allergens in latex, seem to be advantageous for promoting the sulfur curing of NR (Suchiva *et al.*, 2000; Mai and Yu, 2006). However, these substances can be removed when the latex is subjected to the manufacturing processes.

NR is a linear polymer with glass transition temperature ( $T_g$ ) and specific gravity at 20°C of ~70°C and 0.93, respectively. For this reason, it possesses many versatile properties; for instance, low compression set, low hysteresis, high resilience, and excellent fatigue resistance (Teh *et al.*, 2004; Mai and Yu, 2006). The neat NR also demonstrates a typical strain-induced crystallization behavior; that is, at lower strain region, the modulus is low and increases slowly with the increase of strain. but after approaching a certain value, the stress will rise sharply within a small range of strain due to the appearance and rapid development of tensile crystallization. From the rheological behavior point of view, pure NR displays the pseudoplastic behavior (viscosity decreases with increasing the shear rate) at lower shear rates, whereas at higher shear rates, it in turn shows the Newtonian behavior (viscosity becomes independent of the shear rate) (Stephen *et al.*, 2007). Thus, the commercial applications of NR are in the production of surgical gloves, balloons, tyres, bumpers, etc. However, NR has limited ozone resistance and high dependence of dynamic properties on temperature (Arroyo *et al.*, 2007) and is known as an insulating material.

To optimize the mechanical strength and barrier effectiveness, the pure NR has to be vulcanized, and the most widely used cross-linking agents are sulfur and peroxide. Herein, only sulfur vulcanization will be discussed in detail, as it is the main route used in the present study to cure the foam-like materials based on NR. Besides, the peroxide cured NR are found to have lower strength properties than those obtained by sulfur curing (Mai and Yu, 2006). Sulfur vulcanization method involves activators for the breakage of the sulfur ring ( $S_8$ ) and accelerators for the

formation of sulfur intermediates, which facilitates sulfur to double bond cross-linking. Without any accelerators, the sulfur vulcanization reaction takes several hours and is of no commercial importance, while by using accelerators, the optimum curing time can be reduced to as short as 2–5 min. Once being cured, three different types of sulfur bridges are generated; that is, polysulfidic ( $S_x$ ), disulfidic ( $S_2$ ), and monosulfidic (S) linkages. The distribution of these bridges depends primarily on the level of sulfur and the ratio of accelerator to sulfur (Mai and Yu, 2006). The polysulfidic linkages mainly appear within the conventional (CV) system (lower accelerator to sulfur ratio), while the mono or disulfidic linkages are predominantly formed in the efficient (EV) system (higher accelerator to sulfur ratio). It is the latter that often displays more heat resistance than the former linkage, although the tensile strength and fatigue resistance are better with the polysulfidic linkage (Kurian *et al.*, 1988). It should be noted that both the quantity and quality of sulfur linkages play the dominant role on the mechanical performances of the rubber vulcanizates.

The neat NR can be vulcanized without the need of free sulfur through the reaction with sulfur compounds (Akiba and Hashim, 1997). This means that the actual cross-linking agents are the activated sulfur atoms, which are released from the sulfur-donor compounds such as sulfur monochloride ( $S_2Cl_2$ ), bis-mercaptans, thiourea derivatives, etc.  $S_2Cl_2$  is known as a cold vulcanization agent for NR, since it will vulcanize NR so fast even at very low temperatures that the rubber cannot be mixed into rubber compounds. Thus, its use as a cross-linking agent is less common. However, previous works (Okay *et al.*, 2000; Ceylan *et al.*, 2007; Dogu and Okay, 2008; Tuncaboylu and Okay, 2009; Ceylan *et al.*, 2009) have shown that  $S_2Cl_2$ , being a liquid at room temperature and soluble in organic solvents, was an effective cross-linker for the solution cross-linking process of butyl rubber (PIB), even at very low polymer concentrations. The organogels thus obtained displayed the distinct characteristics in terms of internal morphology, degree of toughness and rate of response against the external stimuli (solvent change), that strongly depend on a large number of factors such as preparation temperature ( $T_{prep}$ ), freezing rate, choice of a cross-linking medium, and concentration of  $S_2Cl_2$ . For instance, the gel particles prepared under frozen state conditions using benzene as the cross-linking medium exhibited the macro-porous structure, consisting of large interconnected pores, with

superfast responsivity and high degree of toughness, through which they can be compressed up to 100% strain without any crack development.

### 2.2.2 Nanocomposites Formation and Their Structures

Since the early days of the rubber industry, carbon black (CB) is the most widely used reinforcing filler especially in tire industry, in which it serves as fillers for improving tear strength, modulus, and wear characteristics of the tires (Praveen *et al.*, 2008). Because of its origin from petroleum, the preparation and processing of CB is hazardous, and it produces a black color to rubber. Thus, many attempts have been made to replace CB with other reinforcing agents in the formulation of rubber compounds such as precipitated silica, kaolin, and sepiolite. As these inorganic fillers are incompatible with the rubber matrices, their reinforcing efficiency was inferior as compared to that of CB, and more importantly they often reduce the crosslink density of the rubber vulcanizates (Mai and Yu, 2006; Praveen *et al.*, 2008).

In the meantime, the layered silicate nano-fillers have already been developed. Owing to the natural occurrence and beneficial properties of Na<sup>+</sup>-MMT in terms of a high specific surface area, aspect ratio, and cation exchange capacity, the elastomer nanocomposites based on various types of rubber have attracted a considerable attention and interest of many academic and industrial researchers. The addition of only a low percentage of layered silicates ( $\leq 5$  wt%) can significantly improve the mechanical, flame resistance, thermal endurance, and barrier properties of the rubber matrix. These superior performances are explained in terms of the nanometer scale of the dispersed silicate layers and the high interfacial adhesion between the matrix and silicate layers, as opposed to the conventional composites.

To date, there are four major techniques for preparing the elastomer nanocomposites. The detail of each process is given below (Mai and Yu, 2006):

#### (i) *In-situ polymerization*

The silicate layer is first swollen within the monomer solution or liquid monomer so that the polymer can be formed inside the interlayer spacing. The polymerization is then initiated either by heat or radiation, by adding the initiator, or by a catalyst situated inside the clay galleries.

(ii) *Intercalation via solution*

This is based on a solvent system, in which the polymer is soluble, and the clay can be swellable. The silicate layer is first swollen in the solvent, followed by mixing with the rubber solution so that the rubber chains intercalate and replace the solvent within the clay galleries. Upon solvent removal, the silicate layers reassemble around the rubber phase, leading to the formation of elastomer nanocomposites.

(iii) *Direct melt intercalation method*

This is the most promising method as compared to the others since it is feasible with current industrial process, economic favorable, and environmentally benign due to the absence of solvents. The process involves annealing a mixture of the polymer and organically modified layered silicate (OMLS) above the softening temperature of the polymer under the shear force. As a result, the polymer chains diffuse from the molten mass into the interlayer spacing to form either intercalated or exfoliated nanocomposites.

(iv) *Latex compounding*

This is also another promising method in preparing the elastomer nanocomposites due to the simplicity of technique itself and superior cost/performance ratio compared to the solution intercalation (Wu *et al.*, 2005). This process begins with dispersing the pristine clay in water that acts as a swelling agent, as previously described in section 2.1. Then, the rubber latex is added and mixed with clay suspension for a period of time, followed by coagulation using the electrolyte solution e.g. calcium chloride aqueous solution to attain the elastomer nanocomposites.

Optimizing the interfacial contact area between rubber matrix and the reinforcing agents like silicate layers is the most important issue for the creation of the nanocomposites. Those interactions generally affect the macroscopic properties of the produced materials and can be fine-tuned by properly controlling the surface chemistry of the silicate layers or bonding types between the rubber matrix and silicate layers (Chrissopoulou *et al.*, 2005; Kellarakis *et al.*, 2007). On the basis of the strength of this interfacial interaction, four different configurations of the elastomer nanocomposites can be produced, as depicted in Figure 2.8: (i) phase separated

structure (known as the conventional composite), where the rubber matrix does not intercalate between the silicate layers, and the clay particles act as the micron-sized fillers, (ii) intercalated structure, where the rubber chains intercalate into the galleries and maintain the parallel registry of pristine silicates, (iii) exfoliated structure, where the periodicity or parallel stacking is lost, and the silicate layers are dispersed individually within the rubber matrix, and (iv) intermediate structure, where both the intercalated and exfoliated configurations are present. As a matter of fact, it is the exfoliated configuration that is of particular interest, as the fully delaminated silicate layers maximize the interfacial adhesion with the rubber matrix and promote the formation of micro-cracks, crack deflection, and the ability to withstand the applied load (Soundararajah *et al.*, 2009).

The thermodynamics of intercalation or exfoliation have already been discussed in terms of enthalpic (H) and entropic (S) contributions to the Gibb free energy (G) (Mai and Yu, 2006; Chrissopoulou *et al.*, 2005). Although there is an entropy loss upon the intercalation of rubber chains within the interlayer spacing, the process is allowed since there is an entropy gain associated with either the increased conformational freedom of the surfactant tails, the desorption of solvent molecules, or the layer separation. Therefore, a net entropy change is close to zero. Thus, the nanocomposites formation and their structure depend primarily on the favorable of enthalpic interactions, which can be determined from the surface energies of the polymer and silicate layers.



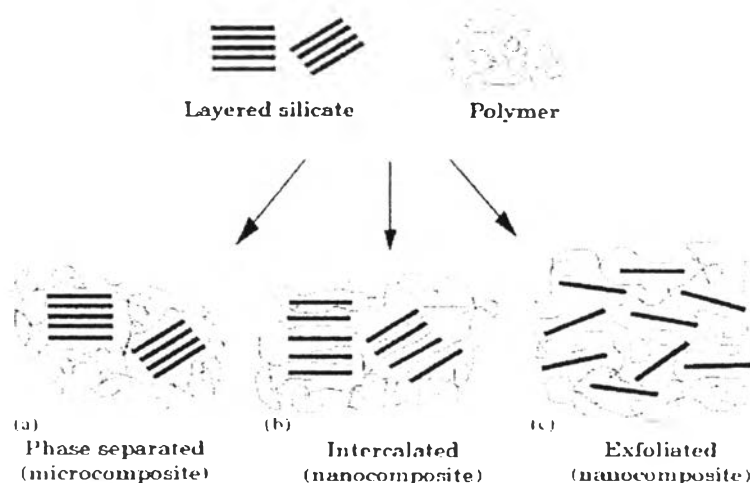


**Figure 2.8** Scheme of different types of composite arising from the interaction between layered silicates and polymer matrices (Alexandre and Dubois, 2000).

Varghese and Kocsis (2003a) prepared the NR-based nanocomposites by latex compounding with sodium bentonite and sodium fluorohectorite. The elastomer nanocomposites exhibited a great increase in tensile strength, storage modulus and thermal stability, particularly when using the sodium fluorohectorite. This was attributed to the reinforcing effect, imparted by intercalated or exfoliated sheets and formation of a skeleton structure.

The same authors (2003b) utilized the melt compounding method for preparing the elastomer nanocomposites comprising pristine or organophilic layered silicates. It was observed that the organophilic clays accelerated the sulfur curing of NR through the formation of a zinc coordination complex in which both sulfur and amine groups of intercalants participated. This led to the collapse of the interlayer spacing. The high-temperature relaxation of NR matrix was explained by a part of the rubber chains situated in the confined regions.

López-Manchado *et al.* (2003) studied the effect of bentonite and its organically modified form on the vulcanization kinetics of NR through cure-meter tests and thermal analysis under dynamic and isothermal conditions. The addition of organoclay resulted in a marked decrease in induction and cure time of the elastomer nanocomposites as compared to those of the composites comprising the neat

bentonite. Also, a drastic increase in torque value signified the formation of effective crosslinks, as explained by a good interaction between the two components and confinement of rubber chains within the interlayer spacing. Based on the calculated activation energy, it was concluded that the organoclay improved the rubber processability, as a lower energy was required for the cross-linking reaction.

Wang *et al.* (2003) introduced the elastomer nanocomposites prepared by co-coagulating the mixture of rubber latex and clay solution with 2% dilute sulfuric acid. X-ray diffraction (XRD) and electron microscopy (TEM) analyses showed that the rubber molecules did not intercalate into the clay galleries but rather separated the particles into either clay aggregates with ~10-20 nm thick or individual layers. Although the elastomer nanocomposites displayed a high hardness, modulus, tear strength, and gas barrier properties, a typical strain-induced crystallization behavior of rubber was inhibited.

Stephen *et al.* (2006a) studied a rheological behavior of the elastomer nanocomposites with respect to shear rate, clay loading, and temperature. The viscosity of rubber latex increased as a function of clay loadings due to the network formation between rubber and silicate layers and more uniform dispersion of clay particles on nanoscale. Further, the filled rubber latex possessed a more pseudoplasticity than the neat rubber latex owing to the breakdown of network structure upon increasing the shear rate. Because of the collapse of such network, the viscosity of the filled latex also decreased with increasing temperature.

The same authors (2006b) studied the gas transport through micro and nano composites of NR latex membranes produced via latex compounding. The authors reported that the nano-filled composites exhibited reduced permeability to oxygen and nitrogen gases compared to micro-filled composites. This was attributed to the platelet like morphology and high aspect ratio of layered silicate, which results in more tortuous path for the permeant molecules to pass through the membranes. In contrast, the micro-filled composites showed higher permeability because of the lack of good interaction between polymer and filler causing the formation of filler aggregation at high loading and micro cavities at the interface region.

Avalos *et al.* (2008) investigated the influence of intercalants i.e. aromatic and aliphatic on the cure characteristics of NR. The authors found that the

aliphatic salt gave a higher interlayer separation of Na<sup>+</sup>-MMT compared to the aromatic one and facilitated the intercalation of rubber chains. This led to the superior mechanical behaviors as well as the existence of exfoliated structure. Curing studies indicated that the aliphatic-MMT clay was capable of catalyzing the cross-linking reaction, and this was reflected in the lowest and highest values of activation energy and torque, respectively.

### 2.3 Electrically Conducting Polymers (CPs)

Electrically conducting polymers (CPs), polypyrrole (PPy), polyaniline (PANI), polythiophene, and others, have attracted a great deal of interest because of the conjugated electronic structure and unique electronic properties. To this regard, they are promising for a wide variety of advanced applications such as anti-static and anti-corrosion coating, sensors, batteries and supercapacitors, light emitting diode (LEDs), transparent electrode materials, and electrochromic devices (Sadki *et al.*, 2000). The electrical conductivity of CPs is explained by the electron moving or hopping (delocalization) along and across the conjugated polymer backbone. As a consequence, the higher the charged species (electron holes) formed along the main chain, the greater the electrical conductivity of the final materials. Further, the CPs having a longer chain and a more co-planarity between interchains are favorable for a higher conductivity performance (Liu and Ger, 2002). The electrical conductivity of CPs can be dramatically improved through an oxidation (p-type doping: removal of electrons from  $\pi$  orbital by an oxidizing agent, leaving behind polymeric cation) or a reduction (n-type doping: donation of electrons to the  $\pi$  orbital by a reducing agent, leaving being polymeric anion). This is followed by the insertion of anionic or cationic species into the CPs backbone, respectively. Owing to the double bond alternation in the conjugated polymer chain, the charged species formed upon doping are capable of moving along the carbon chain (delocalization), thus giving rise to the electronically conductive material (Sadki *et al.*, 2000).

Among the numerous CPs known to date, polypyrrole (PPy) is by far recognized to be one of promising CPs for various commercial applications, since it presents a number of advantages including high electrical conductivity, good redox

properties, environmental stability to oxygen and water, relative ease of synthesis, and the ability to form composites with the appreciable chemical and physical properties (Sadki *et al.*, 2000; Hong *et al.*, 2001; Liu and Ger, 2002; Kim *et al.*, 2003; Omastová *et al.*, 2003). Similar to the general CPs, PPy can be synthesized via either chemical or electrochemical polymerization of pyrrole monomer in various organic solvents or in aqueous media. In fact, it is the latter method that is generally preferred, as it provides a better control of film thickness and microstructure, better conducting properties, and more cleaner polymer, as compared to the chemical oxidation (Sadki *et al.*, 2000; Omastová *et al.*, 2003).

The electrical conductivity of PPy synthesized by chemical oxidative polymerization varies in the range between  $10^{-4}$  and  $100 \text{ Scm}^{-1}$ , depending on the experimental conditions, temperature, and various additives introduced into the reaction mixture (Boukerma *et al.*, 2006). Many oxidants have been utilized for initiating the chemical polymerization of pyrrole; for instance, ferric chloride, ferric perchlorate, and ammonium peroxydisulfate. Generally, the ferric chloride ( $\text{FeCl}_3$ ) is used as oxidant in PPy synthesis (see Figure 2.9), as it gives the conducting polymer with highest conductivity compared to the others. The optimum  $\text{FeCl}_3$ /pyrrole molar ratio is at 2.3 (Omastová *et al.*, 2003). Additives like anionic surfactants e.g. sodium dodecylbenzenesulfonate (DBSA), sodium dodecyl sulfate (SDS), sodium bis(2-ethylhexyl) sulfosuccinate (AOT), etc. can enhance the electrical properties of chemically synthesized PPy. This is explained by the fact that a part of anionic surfactant is incorporated into the PPy polycation through ionic bonding similarly as the anion of oxidant and modifies the parameters of the conducting network as well as the chain regularity during the polymerization (Omastová *et al.*, 2003). In other words, anionic surfactant is now acting as a dopant introducing charge carriers in the form of polaron (radical cation) or bipolaron (dication) within the polymer backbone (see Figure 2.10). However, a very bulky aliphatic chain of surfactant can be a steric barrier for the charge transport along the PPy backbone and hence decrease the electrical conductivity (Omastová *et al.*, 2003). Note that a polaron is formed after losing an electron from the neutral polymer chain, while a bipolaron is created upon the removal of another unpaired electron.

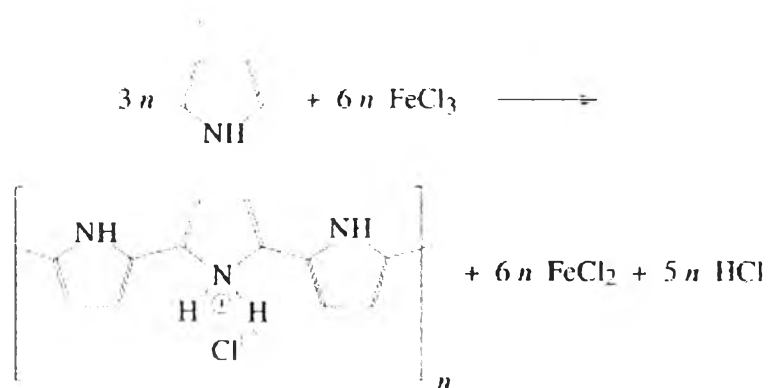


**Figure 2.9** Chemical oxidative polymerization of pyrrole with  $\text{FeCl}_3$  (Omastová *et al.*, 2003).

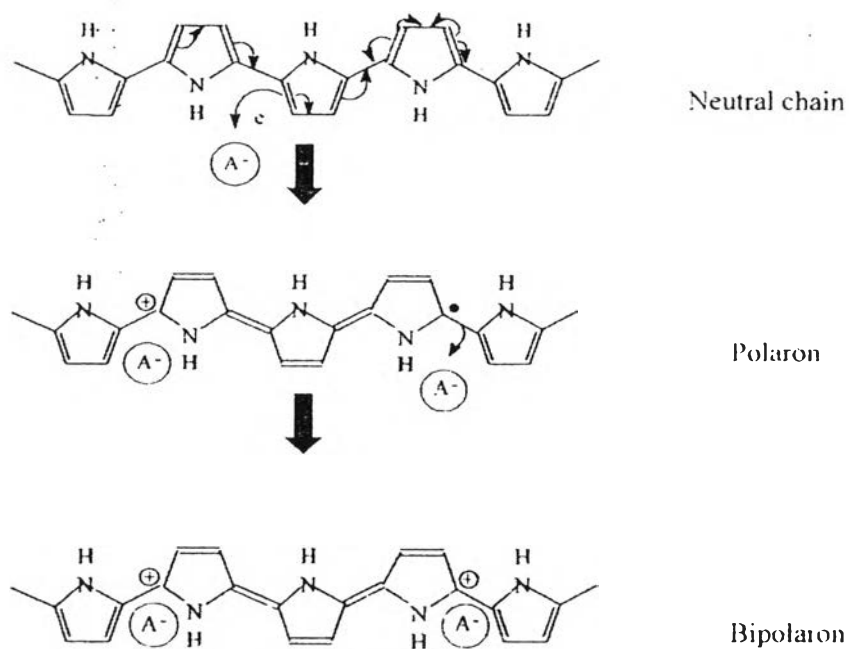


**Figure 2.10** The formation of polarons and bipolarons upon doping the PPy backbone (Chirasakulkarun, 2008).

Regarding the electrochemical polymerization, three different techniques can be utilized for conducting the electropolymerization of pyrrole monomer: potentiostatic (constant potential), galvanostatic (constant current), or potentiodynamic (cyclic voltammetry) methods. The constant potential and current

methods have been commonly utilized to investigate the nucleation mechanism and macroscopic growth, while the cyclic voltammetry mainly provides the qualitative information regarding the redox processes and the electrochemical behavior of the conducting film after the electro-deposition (Sadki *et al.*, 2000). Typically, the pyrrole monomer is first dissolved in an appropriate solvent containing the desired anionic dopant, followed by being oxidized at the surface of an electrode by application of an anodic potential (anodic oxidation). At the end of the reaction, the polymeric film with controllable thickness is formed at the anode (Sadki *et al.*, 2000). This anode electrode can be made of a wide variety of materials such as platinum, gold, copper, glassy carbon, and tin or indium-tin oxide (ITO) coated glass. The selectivity of solvent and electrolyte as well as reaction temperature are of particular important in electrochemistry as compared to the other parameters i.e. monomer substitution, acidity or pH, and applied potential, as their nature has a strong influence on the quality of the PPy films in terms of morphological, electrical and mechanical properties.

There are a large number of the electropolymerization mechanisms proposed to date; however, the mechanism proposed by Diaz and his colleagues is certainly the most probable. They have demonstrated a combination of several successive reactions, starting with a radical cation formation of pyrrole monomer upon the initial oxidation, followed by radical coupling with other monomers and deprotonation until the final polymer product is achieved. This is depicted in Figure 2.11. The electropolymerization does not give the neutral conducting polymer but instead the oxidized conducting form (doped state), as the final polymer contains one protonated nitrogen per three to four pyrrole units, which is electrically compensated by the electrolyte anion (~ 35% in weight as compared to ~ 65 wt% of polymer). It is worth-noting that the synthesis and doping of the conducting polymer are conducted simultaneously during the electropolymerization.

Unfortunately, both the chemically and electrochemically synthesized conducting PPy are brittle, insoluble in water and common organic solvents, infusible, and thus not processable. Therefore, many attempts have been devoted to the development of conducting polymer composites comprising various inorganic particles: for instance, Na<sup>+</sup>-MMT clay (Hong *et al.*, 2001; Liu and Ger, 2002; Kim *et*

*al.*, 2003; Boukerma *et al.*, 2006; Mravčáková *et al.*, 2006), mesoporous silica (Cheng *et al.*, 2006a), ferric oxide ( $\text{Fe}_2\text{O}_3$ ) (Gangopadhyay and De, 1999), yttrium oxide ( $\text{Y}_2\text{O}_3$ ) (Cheng *et al.*, 2006b), titanate (TN) nanowire (Cheng *et al.*, 2008), etc. These composite systems provide the new synergistic properties that cannot be realized from the individual materials. Particularly, the composites of PPy and  $\text{Na}^+$ -MMT are recognized as the potential conductive fillers for modifying the mechanical and conducting behaviors of the other insulating polymer matrices. The rationale is that when the corresponding composites are exfoliated, the conductive paths can be created within the insulating polymer matrix at a low conductive polymer loading (Boukerma *et al.*, 2006). Further, the conductivity of composites comprising PPy and clay varies in the range between  $10^{-7}$  to  $10^{-3} \text{ Scm}^{-1}$ , depending on the weight fraction of conducting polymer, types of oxidant used, and methods of preparation (Mravčáková *et al.*, 2006).

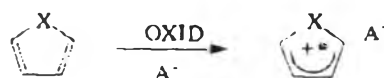
Liu *et al.* (2002) prepared the PPy/ $\text{Na}^+$ -MMT composite through the electrochemical technique on a gold substrate. The surface morphology demonstrated a lamellar and more compact structure as a result of nucleation and growth of the PPy not only on the surface but also within the interlayer spacing. Hence, this led to a significant improvement in electrical conductivity from 26 to  $634 \text{ Scm}^{-1}$  as well as the thermal stability of the nanocomposites as compared to the pristine PPy.

Through emulsion polymerization, Hong *et al.* (2001) successfully prepared the conducting polymer composites comprising the PPy,  $\text{Na}^+$ -MMT clay, and DBSA, acting as emulsifier and dopant. The intercalated configuration was observed through the XRD and TEM analyses. However, it was seen that the PPy-DBSA without clay had a better conducting state as compared to the sample with clay. In other words, the silicate layers interrupted the delocalization of charge carriers and weakened the interaction between the polymerized PPy chains, causing a decrease in the electrical conductivity.

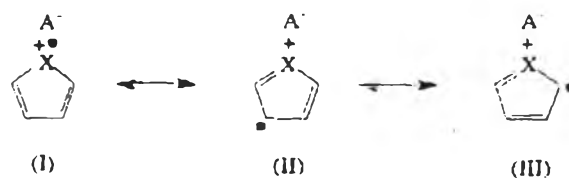
Mravčáková *et al.* (2006) investigated the effect of organic modification of  $\text{Na}^+$ -MMT on the surface composition and electrical properties of the conducting polymer composites, prepared by the chemical oxidative polymerization. It was found that due to the organic modification of clay by the alkylammonium chloride, polymerization of pyrrole at the surface of OMLS was much more efficient in

producing a conductive adlayer, resulting in an enhancement of conductivity of the PPy/OMLS sample ( $1.1 \text{ Scm}^{-1}$ ) as compared to PPy/MMT sample ( $0.031 \text{ Scm}^{-1}$ ). In other words, the surface of former had a polypyrrole-rich surface, while the latter had a montmorillonite-rich surface with the polymerized PPy chains being essentially confined within the clay galleries.

### Step 1. Monomer Oxidation



Resonance forms:



### Step 2. Radical-Radical Coupling



### Step 3. Deprotonation/Re-Aromatization



### Step 4. Chain Propagation

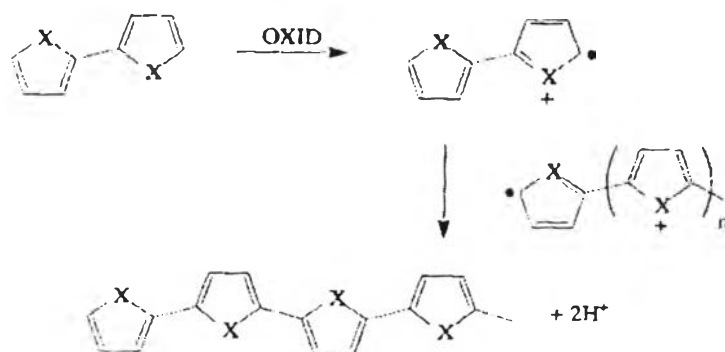


**Figure 2.11** Electrochemical polymerization of pyrrole (Chirasakulkarun, 2008).



## 2.4 Admicellar Polymerization

### 2.4.1 Fundamental of Surfactants

A surfactant, known as a 'surface-active agent', is a substance that has the property of adsorbing onto the surfaces or interfaces of the system and of altering the surface or interfacial free energies of those surfaces and interfaces, respectively, when presenting at very low concentration (Rosen, 2004). Its molecular structure consists of lyophilic and lyophobic group, which is termed as a solvent-loving and solvent hating, respectively. This is known as an amphipathic structure. The chemical structures of groupings suitable as the lyophobic and lyophilic portions of the surfactant molecule vary with the nature of solvent and conditions of use. For instance, in a polar solvent e.g. water, ionic or highly polar group acts as lyophilic groups, while in a nonpolar solvent e.g. heptane, they act as lyophobic groups instead. Upon changing the temperature and conditions of use, modifications of their structure may become necessary in order to maintain their surface activity. The hydrophobic group is usually a long chain hydrocarbon residue, but the hydrophilic group is an ionic or highly polar group.

Regarding the nature of the hydrophilic groups, surfactants can be distinguished as (Rosen, 2004): (i) anionic surfactant: the surface-active portion of the molecule bears a negative charge e.g.  $\text{RCOO}^-\text{Na}^+$  (soap), etc.; (ii) cationic surfactant: the surface-active portion of the molecule bears a positive charge e.g.  $\text{RN}(\text{CH}_3)_3^+\text{Cl}^-$  (quaternary ammonium chloride), etc.; (iii) zwitterionic surfactant: the negative and positive charges are present in the surface-active portion e.g.  $\text{RN}^+\text{H}_2\text{CH}_2\text{COO}^-$  (long-chain amino acid), etc.; and (iv) nonionic surfactant: the surface-active portion contains no ionic charge e.g.  $\text{R}(\text{OC}_2\text{H}_4)_x\text{OH}$  (polyoxyethylenated alcohol), etc. The adsorption of surfactants onto solid-liquid interfaces strongly depends on the nature of surfaces; for example, if the surface is negatively charged, the cationic surfactant will adsorb onto the surface with its positively charged hydrophilic head group oriented towards the negatively charged surface and its hydrophobic group oriented away from the surface, making the surface water-repellent. However, if the surface is made to be hydrophilic, then the cationic surfactants should be avoided. Further, zwitterionics can adsorb on both the

negatively charged or positively charged surfaces without changing the surface charge significantly.

#### 2.4.2 Adsorption at Solid–Liquid Interface

A fundamental characteristic of surfactants is the ability to adsorb at interfaces in an oriented fashion, which is very important for their performances in terms of the interfacial processes; for example, foaming, wetting, dispersion, detergency, and emulsification. The orientation and packing of the surfactant at a particular interface influence the hydrophobicity of such interface; that is, whether it will become more hydrophobic or more hydrophilic. The adsorption of surfactants at solid–liquid interface is strongly dependent on a number of factors: (i) the nature of structural groups on the solid surface—whether it contains the highly charged sites or essentially nonpolar groupings; (ii) the molecular structure of surfactant being adsorbed—whether it is ionic or nonionic, and whether the hydrophobic group is short or long, straight chain or branched, aliphatic or aromatic; and (iii) the environment of the aqueous phase—its pH, electrolyte content, temperature, and the presence of any additives (Rosen, 2004). As a consequence, a number of mechanisms by which the surfactant may adsorb onto solid substrates from aqueous solution have been proposed and given as follows: ion exchange, ion pairing, acid–base transition, adsorption by polarization of  $\pi$  electrons, adsorption by dispersion forces, and hydrophobic bonding (Rosen, 2004). These surfactant aggregates, termed hemimicelles and admicelles, when in the form of monolayers and bilayers, respectively, were assumed to be more or less flat and are readily distinguished from micelles in the solution phase, as shown in Figure 2.12.

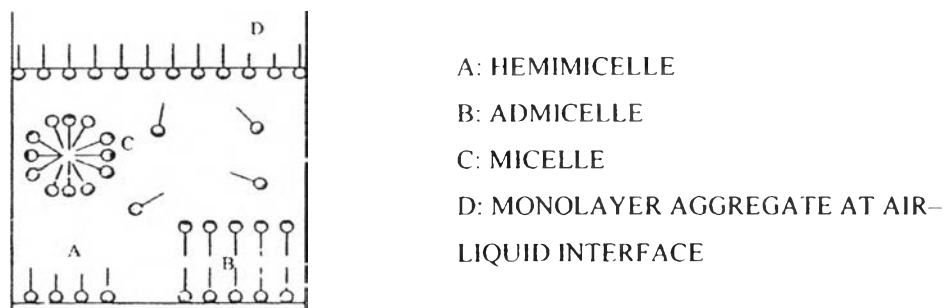


**Figure 2.12** Types of surfactant aggregates.

An adsorption isotherm is often used as a means of describing the adsorption of the surfactant at the solid-liquid interface. In other words, it is a mathematical expression relating the concentration of surfactant, termed 'adsorbate', at the interface to its equilibrium concentration in the liquid phase:

$$n_1^s = \frac{\Delta C_1 V}{m}, \quad (1)$$

$$\Gamma_1 = \frac{n_1^s}{a_s}, \text{ and} \quad (2)$$

$$a_1^s = \frac{10^{16}}{N \Gamma_1}, \quad (3)$$

where  $n_1^s$  is the number of mole of adsorbed surfactant per gram of solid adsorbent at equilibrium (mol/g),  $\Delta C$  is the molar concentration difference of surfactant before ( $C_{1,0}$ ) and after ( $C_1$ ) equilibrium adsorption in liquid phase ( $\text{molL}^{-1}$ ),  $m$  is the mass of the adsorbent (g),  $V$  is the volume of liquid phase (L),  $\Gamma_1$  is the surface concentration of the surfactant ( $\text{molcm}^{-2}$ ),  $a_s$  is the surface area per unit mass of the adsorbent ( $\text{cm}^2\text{g}^{-1}$ ),  $a_1^s$  is the surface area per adsorbate molecule on the adsorbent ( $\text{\AA}^2$ ), and  $N$  is the Avogadro's number ( $6.023 \times 10^{23}$ ). The area per molecule of SDS at surface saturation is equal to  $53 \text{ \AA}^2$  at room temperature (Rosen, 2004).

The adsorption isotherm is then attained from a plot between  $\log \Gamma_1$  and  $\log$  equilibrium concentration of the adsorbate ( $C_1$ ) (see Figure 2.13). It should be noted that the  $n_1^s$  of bilayer coverage is about 2 times higher than that of

monolayer coverage. and the area per molecule at the interface provides information regarding the degree of packing and the orientation of the adsorbed surfactant molecule. For the adsorption of ionic surfactants onto the oppositely charged solid substrate, the adsorption isotherm is typically an S-shaped graph, which can be differentiated into four regions. In region I, the surfactant adsorption is mainly by an ion exchange mechanism, and the amount of adsorbed surfactant increases linearly with its equilibrium concentration. In region II, there is a marked increase in the slope of the isotherm, being a result of interaction between the hydrophobic chains of oncoming surfactant and those of previously adsorbed surfactant to form admicelles (or bilayer aggregates) on the solid surface. The changing point from region I to II is defined as 'critical admicelle concentration (CAC)'. In region III, as the adsorption now must overcome electrostatic repulsion between the oncoming ions and the like-charged headgroups of surfactants on solid surface, the slope is now being decreased. In region IV, the adsorption level approaches a saturation point, in which the amount of adsorbed surfactant remains constant with a further increase in surfactant concentration. The changing point from region III to IV is called 'critical micelle formation (CMC)', the concentration at which the monomeric form of surfactant aggregates to form a cluster, known as a micelle'. Therefore, this plateau region illustrates the micelles formation. In admicellar polymerization, the surfactant concentration is chosen to be in the region III to attain the maximum admicelle formation with no micelles in the solution to avoid the emulsion polymerization (Pongprayoon *et al.*, 2002).

The charge on the substrate surface can be manipulated to be either positive or negative by adjusting the pH of the solution. The solution pH at which the surface exhibits a net surface charge of zero is called 'point of zero charge (PZC)'. At pH below PZC, the surface becomes protonated and more positively charged, while at pH above PZC, the surface is negatively charged. For this reason, anionic and cationic surfactants will adsorb on substrate at pH below PZC and above PZC, respectively. Further, the addition of neutral electrolyte e.g. sodium chloride helps to reduce the charge on the substrate surface as well as the repulsion between the charges on the headgroups of the oncoming ions (Pongprayoon *et al.*, 2002). As a

result, the adsorption of anionic surfactant on the surface will be enhanced due to a much closer packing of surfactant molecules.

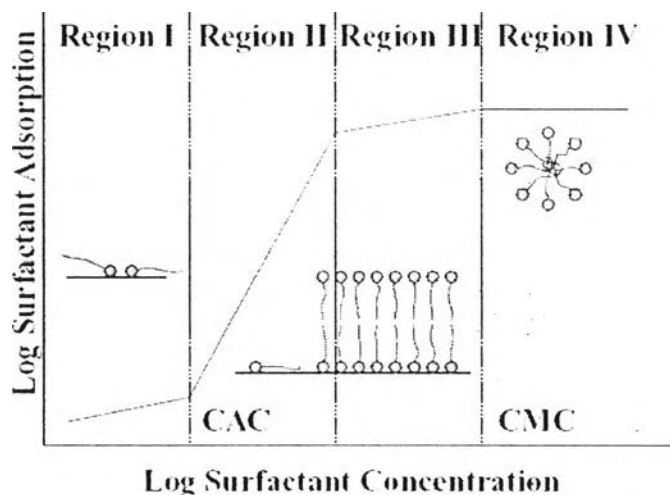


**Figure 2.13** Typical adsorption isotherm of surfactants on a solid surface (Pongprayoon *et al.*, 2002).

When the attraction between the hydrophobic groups is insufficient to overcome the mutual repulsion of the ionic hydrophilic groups (when the hydrophobic groups are short or there are more than two similarly charged ionized groups in the surfactant molecule), then the aggregation of the hydrophobic chains may not occur, and region II may be absent. This leads to an inverted L-shaped isotherm with the adsorption in region I continuing by ion exchange and ion pairing mechanisms until the original charge of the substrate has been neutralized (Rosen, 2004). Then, the adsorption will continue in the same manner as for region III of the S-shaped curve.

#### 2.4.3 Admicellar Polymerization Process

Admicellar polymerization is, by design, a fine-coating technique that creates an ultrathin polymeric film on various kinds of substrates in order to modify their surface properties. The process employs a surfactant bilayer physically adsorbed onto the substrate surface as a 2-dimensional template for *in situ*

polymerization of organic monomers (Bunsomsit, *et al.*, 2002; Pongprayoon *et al.*, 2002). Admicellar polymerization has been used to date for a wide variety purposes; for instance, electropolymer coating on rubber particles and mica flakes (Genetti *et al.*, 1998; Bunsomsit, *et al.*, 2002), hydrophobicity coating on cotton fabric and sisal fiber (Pongprayoon *et al.*, 2002, 2005, 2008), and hydrocarbon component coating on calcium carbonate particles (Rungruang *et al.*, 2006). Besides, the ultrathin polymeric film is capable of increasing the interfacial adhesion between two materials that are heterogenous in nature. Compared to the other thin-film coating techniques e.g. chemical vapor deposition, plasma polymerization, electrochemical deposition, and so on, admicellar polymerization is quite simple with low energy consumption, as the polymerization is conducted in an aqueous surfactant solution without requiring any special equipment, while the monomer may be a gas, liquid or solid (Pongprayoon *et al.*, 2002).

Admicellar polymerization generally consists of four main steps: admicelle formation, monomer adsolubilization, polymer formation, and surfactant removal, as illustrated in Figure 2.14:

(i) *Admicelle Formation*

The formation of the surfactant bilayer on a substrate occurs at a concentration just below the CMC (see Figure 2.13). In the outer surfactant layer, the molecules are oriented with their hydrophilic head groups in contact with the aqueous phase, while the hydrophobic tails interact to form a hydrophobic core. An inner layer oriented with the head groups in contact with the substrate completes the bilayer coverage.

(ii) *Monomer Adsolubilization*

When the organic monomers are introduced into the reaction mixture, they will be preferentially adsorbed in the core of the admicelle in a process termed 'adsolubilization'. This process can occur either after the admicelle formation or simultaneously with the surfactant adsorption.

(iii) *Polymer Formation*

Upon the addition of an initiator (water soluble initiators), the organic monomers in the admicelle undergo a polymerization reaction to form a polymeric layer on the substrate surface.

(iv) *Surfactant Removal*

After the end of reaction, the upper layer of surfactant will be removed as much as possible by washing in order to expose the polymeric layer on the substrate surface. The polymeric film produced via this process can be controlled by several parameters including the characteristics of substrate surface, types of surfactant, monomer molecule, the electrolyte, and the pH value (Pongprayoon *et al.*, 2008).

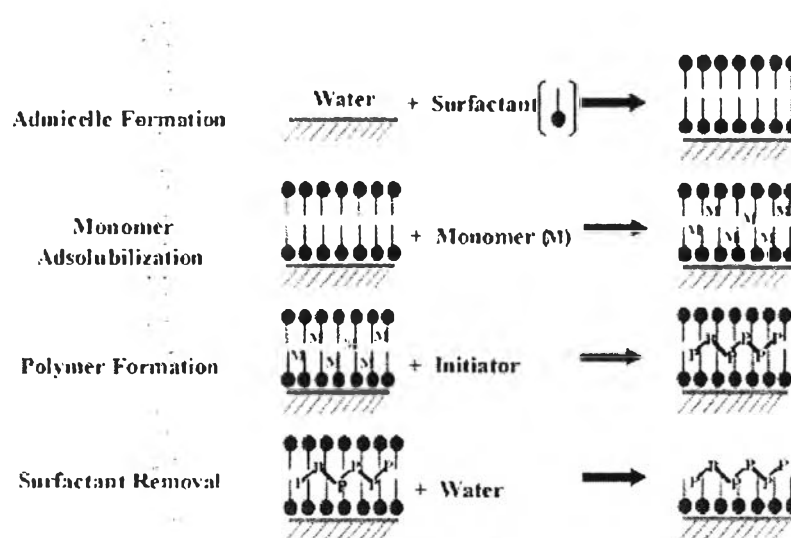


**Figure 2.14** Schematic illustration of the admicellar polymerization process (Rungruang *et al.*, 2006).

Genetti *et al.* (1998) discovered that via admicellar polymerization, coating of nickel particles with PPy increased the electrical conductivity of the nickel-filled low-density polyethylene (LDPE) composites by three orders of magnitude at concentrations well above the percolation threshold. This was explained by the formation of molecular wires created by PPy entanglements, which reduced the particle–particle contact resistance as well as the tunnelling resistance. Further, the mechanical and thermal properties of the corresponding composites were not affected by the addition of PPy coating to the nickel particles due to the immiscibility between PPy and LDPE.

Pongprayoon *et al.* (2002) demonstrated that polystyrene (PS) coating via admicellar polymerization increased the hydrophobicity of cotton fabric, as determined by a time for water droplet to disappear. Further, the water repellency of the treated cotton was found to be dependent on the surfactant: monomer and monomer: initiator ratios; that is, the higher the concentration of initiator (more PS formed), the greater the hydrophobicity of the treated fabric.

Bunsomsit *et al.* (2002) found that the coating of NR latex particles with PPy via admicellar polymerization facilitated both the processing of pristine PPy and improved the electrical conductivity of the rubber latex by seven orders of magnitude. The addition of sodium chloride increased the monomer adsorption in the SDS admicelles by reducing the repulsion between the hydrophilic head groups. Thus, the conductivity was further increased by as much as 2x due to the more connectivity of PPy.

Chirasakulkarun *et al.* (2008) introduced the electrochemical method for forming the ultrathin PPy film around the rubber latex particles using the SDS bilayer as a reaction template. The authors investigated the influence of applied voltages and monomer concentrations on the polymerization process and found that a reaction time was decreased with an increase in the voltage from 6 to 15 volts; however, a voltage higher than 9 volts showed the corrosion effect on the copper electrodes, particularly at 15 volts. Further, as the pyrrole content was increased from 20 to 800 mM, the higher polymerization rate as well as the superior thermal, mechanical, and electrical behaviors was realized.